FUDMA Journal of Renewable and Atomic Energy (FJoRAE)
ISSN: 3027-2335
Vol. 2 No June 2025. Pp 67-84

https://doi.org/10.33003/fjorae.2025.0201.05

Effect of Chord Length on the Aerodynamic Performance of VAWTs with NACA 0015 Airfoil at Low Wind Speeds.

Ogunsesan, A.A[11*], Muhammed, S.U[2] and Oluwole, W[3]
[1,2,] Department of Mechanical Engineering, Nigerian Defence Academy, Kaduna Nigeria
[3]Department of Aerospace Engineering, Airforce Institute of Technology, Zaria.

ABSTRACT
The aerodynamic performance of Vertical Axis Wind Turbines (VAWTs) in low-wind regions is strongly influenced by blade geometry, with chord length playing a key role in optimizing energy capture. Despite their low performance challenges, VAWTs remain a viable option for harnessing wind energy in urban and low-wind-speed environments. The NACA 0015 airfoil has been widely recommended by many studies for its effectiveness under such conditions. However, few studies have specifically investigated the impact of chord length on the performance of VAWTs using the NACA 0015 airfoil, despite numerous optimization efforts. This study investigates the influence of blade chord length on the aerodynamic performance of VAWT employing the NACA 0015 airfoil under low wind speed conditions, specifically 3m/s and 4m/s. Using 2D transient CFD simulations with the SST k-ω turbulence model, three chord lengths (0.1 m, 0.2 m, and 0.3 m) were assessed over a Tip Speed Ratio (TSR) range of 2.0 to 4.5. The findings from this study showed that chord length plays a dominant role in the performance of a VAWT in low wind regimes. While the configuration with 0.1m chord length generated the maximum power coefficient (Cp) of 0.395 during the 4m/s wind speed, the 0.2m chord length configuration produced a more stable performance with a peak Cp of 0.371. At a wind speed of 3m/s, the configuration with 0.3m chord length displayed signs of deteriorating performance due to an excessive increase in solidity. The findings provide insight into optimal chord sizing for small-scale VAWTs operating in urban low-wind environments, supporting design decisions for decentralized wind energy systems.

KEYWORDS

Wind Energy, VAWT, Aerodynamic performance, TSR, CFD, Chord length.

1. INTRODUCTION

The world is moving toward renewable energy alternatives due to the negative effects of fossil fuels on the environment and the economy, including increased emissions, resource depletion, and supply volatility (REN21, 2022; IEA, 2021). Among these, wind energy stands out due to its wide availability, technological maturity, and zero-emission operation (Manwell *et al.*, 2010). However, the dominance of Horizontal Axis Wind Turbines (HAWTs) in large-scale installations comes with limitations, particularly in low wind speed environments, urban areas, and sites with turbulent flow (Islam *et al.*, 2013). Vertical Axis Wind Turbines (VAWTs) present a viable substitute in these situations. They are ideal for decentralized and small-scale applications due to their simple mechanical design, lower installation height, and capacity to receive wind from all directions (Paraschivoiu, 2002; Howell *et al.*, 2010).

Corresponding Author's e-mail[1] ogunsesan.abdulafeez2022@nda.edu.ng

Despite these benefits, VAWT performance is extremely sensitive to aerodynamic design parameters, particularly at low Reynolds numbers where dynamic stall and flow separation are more noticeable (Islam *et al.*, 2013; Howell *et al.*, 2010). Aerodynamic parameters like solidity, the ratio of total blade area to rotor swept area, and tip speed ratio (TSR), the ratio of blade tip speed to incoming wind speed, are essential to comprehending VAWT behavior (Kishore *et al.*, 2021). These variables affect overall efficiency, flow behavior, and torque generation. Furthermore, a crucial geometrical characteristic of the blade, chord length, has a direct impact on the Reynolds number, which in turn influences the formation of the boundary layer and aerodynamic loading (Maalouly *et al.*, 2022; Danao *et al.*, 2014).

While several studies have been conducted on how parameters such as airfoil shape, blade number, and TSR affect the performance of a VAWT, few have been conducted to understand how chord length variations affect aerodynamic performance, particularly under low wind speed conditions and using symmetrical airfoils like NACA 0015. Most existing works either focus on fixed chord designs or evaluate performance under moderate to high wind speeds, leaving a gap in the understanding of how chord length influences flow separation, torque generation, and efficiency in low-Reynolds-number environments.

Several studies have highlighted the importance of selecting a suitable airfoil profile for VAWTs to operate efficiently in low wind conditions. Mohamed *et al.* (2014) performed a numerical investigation of 25 airfoils and identified NACA 0015, among others, as highly suitable for low wind speed applications. Davari *et al.* (2024) compared the performance of symmetric (NACA 0015) and Selig airfoils; the result showed that NACA 0015 achieved a higher peak power coefficient (Cp), though they noted that modifying thickness-to-camber ratio could enhance performance further. Similarly, Subramanian *et al.*, (2017) found that NACA 0015 produced the highest Cp for both two- and three-blade configurations in a CFD analysis. Zhang *et al.* (2021) used CFD to analyze a straight-blade VAWT under turbulent conditions and validated the results against experiments. A peak Cp of 0.225 was recorded at TSR 2.19 with 8 m/s wind speed, and flow separation was found to vary with azimuth angle. Their study provides a reliable CFD model for assessing VAWT performance in complex urban environments. NACA 0015 has consistently been found to be an efficient airfoil for VAWT use at low Reynolds numbers, making it an excellent foundation for investigating further geometric modifications like chord length.

Solidity, which is influenced directly by chord length, has been a key focus in several investigations. Eboibi *et al.* (2016) found that increasing chord length (and hence solidity) improved the Cp of a NACA 0022-based VAWT, with peak Cp reaching 0.34 at TSR 3.75. Du *et al.*, (2019) similarly observed that higher solidity improved self-starting ability but reduced maximum Cp. Lee and Lim (2015) added a detailed view, showing that short chord–large diameter combinations performed better at high TSRs, while long chord–small diameter setups were more effective at low TSRs. Subramanian *et al.*, (2017) also supported the influence of solidity, confirming higher Cp values with increased solidity in simulations using NACA 0015. Ma'alouly *et al.* (2022) conducted a transient CFD analysis on H-type VAWTs, testing chord lengths ranging from 0.2 to 0.8 m, using the NACA 0017 airfoils. According to their findings, at low TSRs, the high solidity turbine showed improved power coefficient and self-starting ability. The study also demonstrated a strong correlation between chord length, Reynolds number, and overall aerodynamic performance, with optimal TSR values shifting lower with higher chord. Chord length, solidity, and performance have a complicated relationship; while an increase in solidity aids self-starting at low TSRs, it may also reduce the peak Cp of the VAWT. Hence, the goal of the current study is to fully optimize this balance for NACA 0015 in low wind conditions.

Other studies have concentrated on the number of blades and turbine configuration. Howell *et al.* (2010) and Castelli *et al.* (2012) demonstrated that three-bladed configurations consistently

outperformed four- and five-bladed ones, achieving higher Cp (up to 0.4 at TSR 2.58 for NACA 0025). Beri *et al.* (2012) also confirmed that three-blade turbines generated more torque and better self-starting capability than two-blade setups. However, Li *et al.*, (2015) reported a conflicting result, suggesting that increasing the number of blades could actually reduce Cp. Despite the general preference for three-blade configurations, there is still some inconsistency in the literature. This demonstrates the need for more targeted research that changes other important factors, like chord length, while maintaining a constant blade number.

Dynamic stall is a well-documented phenomenon in VAWTs, especially under low TSR conditions. Sebastien and Karen (2022) identified three dynamic stall regimes (deep, light, and no stall), providing insight into performance losses. Bangga *et al.*, (2021) found that thicker airfoils can suppress dynamic stall, while De Tavernier (2021) showed that vortex generators (VGs) mitigate unsteady separation under fluctuating flow conditions. Since dynamic stall affects performance under low wind/TSR scenarios, any modification like chord length must be considered. The present study contributes to this area by evaluating how different chord lengths affect flow separation and stall onset for NACA 0015.

Despite an extensive body of literature on blade numbers, airfoil profiles, and TSRs, there remains a specific gap focusing specifically on the effect of chord length on the aerodynamic performance of NACA 0015-based VAWTs under low wind speed conditions. Most prior studies used different airfoils, such as NACA 0022, NACA 0025, but did not explicitly focus on varying chord length while keeping other parameters constant. This study addresses that gap by employing 2D transient CFD simulations using the SST k-ω turbulence model to evaluate the aerodynamic performance of VAWTs with varying chord lengths, all based on the NACA 0015 airfoil. The study examines how chord length affects the power coefficient, torque production across a range of TSR values at low inlet wind speeds. The findings provide practical insights for optimizing small-scale VAWT designs, particularly for deployment in regions with low wind speeds.

2. THEORETICAL ANALYSIS

2.1 Governing Equation

The two main equations of fluid mechanics principle governing the flow of fluid over the VAWT examined in this study are;

i. Continuity Equation

This equation ensures that the mass of fluid entering and exiting the control volume are equal. Since the fluid employed by this study is at low wind speed, the density remains constant, i.e an incompressible flow. The continuity equation is given as;

$$\frac{\partial \rho}{\partial t} + \blacktriangledown.(\rho U) = 0 \qquad (1)$$

Since density, ρ = constant, equation 1 becomes;

$$\blacktriangledown.U = 0 \qquad (2)$$

Where U = velocity vector field

ii. Navier-stokes Equation

When a flowing fluid comes in contact with a solid body, the properties of the fluid, such as velocity, pressure, etc. Changes due to the shape of the body and also velocity of the flowing fluid itself. In order to be able to predict the behaviour of the flowing fluid around the blades over time, the Navier-stokes equation is solved numerically by the CFD software, in order to calculate the performance metrics analyzed by this study. The Navier-Stokes equation is given as;

$$\rho(\frac{\partial u}{\partial t} + u \cdot \nabla u) = -\blacktriangledown P + \mu \blacktriangledown^2 u \quad (3)$$

Where, ρ = fluid density (kg/m^3)

u = velocity vector (m/s)

t = time (s)

▼P = pressure gradient (pa/m)

μ = dynamic viscosity (pa.s)

▼^{2}U = Laplacian of velocity

For a 3D flow in Cartesian coordinates (x, y, z), the equations are:
Momentum equations (x, y, z components):

$$\rho\left(\frac{\partial u}{\partial t} + u\frac{\partial u}{\partial x} + v\frac{\partial u}{\partial y} + w\frac{\partial u}{\partial z}\right) = -\frac{\partial p}{\partial x} + \mu\left(\frac{\partial^2 u}{\partial x^2} + \frac{\partial^2 u}{\partial y^2} + \frac{\partial^2 u}{\partial z^2}\right) + f_x$$

$$\rho\left(\frac{\partial v}{\partial t} + u\frac{\partial v}{\partial x} + v\frac{\partial v}{\partial y} + w\frac{\partial v}{\partial z}\right) = -\frac{\partial p}{\partial y} + \mu\left(\frac{\partial^2 v}{\partial x^2} + \frac{\partial^2 v}{\partial y^2} + \frac{\partial^2 v}{\partial z^2}\right) + f_\gamma$$

$$\rho\left(\frac{\partial w}{\partial t} + u\frac{\partial w}{\partial x} + v\frac{\partial w}{\partial y} + w\frac{\partial w}{\partial z}\right) = -\frac{\partial p}{\partial z} + \mu\left(\frac{\partial^2 w}{\partial x^2} + \frac{\partial^2 w}{\partial y^2} + \frac{\partial^2 w}{\partial z^2}\right) + fz$$

2.2 Key Aerodynamic Concepts and Performance Metrics

i. Tip Speed Ratio (TSR)

This parameter quantifies the relationship between the incoming speed of the air and the rotational speed of the blades. It represents how many times faster the tip of the blades can move compare to the wind speed. The TSR can be calculated using;

$$\boldsymbol{\lambda} = \frac{R\,x\,\omega}{U} \quad (4)$$

Where $\boldsymbol{\lambda}$ = TSR
ω = Angular velocity (rad/sec)
R = Rotor radius (m)
U = wind speed (m/s)

i. Solidity (σ)

It is a dimensionless parameter that affect the amount of the incoming air that the turbine blades can intercept. The solidity increases with chord length, which has theoretical ramifications. Because of the increased blade area interacting with the flow, high solidity improves the torque coefficient (Cm), which is especially advantageous at low tip speed ratios (TSRs). However, due to the increased blockage effects and decreased efficiency, excessive solidity causes aerodynamic interference, increased drag, and a decrease in power coefficient (Cp) at higher TSRs. The solidity is given as;

$$\sigma = \frac{Nc}{D} \quad (5)$$

where N = Number of turbine blades
D = Turbine diameter (m)
c = chord length (m)

ii. Reynold Number

The transition of flow from laminar to turbulent over a body is governed by this dimensionless parameter. It is given as;

$$Re = \frac{\rho U c}{\mu} \quad (6)$$

Where ρ = density of the air
U = wind speed
c = chord length
μ = dynamic viscosity

The chord length of the airfoil has a direct relationship with the Reynolds number. Increasing the chord length directly increases the Reynolds number, thereby altering the properties of the boundary layer. Higher Reynolds numbers promote the transition from laminar flow to turbulent flow, thereby resulting to an increase in lift, whereas lower Reynolds numbers tend to maintain laminar boundary layers, and hence reducing efficiency.

iii. Power Output ($P_{turbine}$)

The power output that can be generated by a VAWT is written mathematically as;

$$P_{turbine} = T \times \omega \quad (7)$$

Where T = Torque produced by the turbine blades
ω = angular velocity of the turbine blades

iv. Power Coefficient (Cp)

The power coefficient is a measure of how efficient a wind turbine is in harnessing energy from the wind. It is calculated using;

$$Cp = \frac{Pturbine}{Pwind} = \frac{T \, x \, \omega}{1/2 \rho A V^3} \quad (8)$$

where T = Torque (Nm)
ω = Angular velocity (rad/sec)
ρ = density of air
A = swept area (m)
V = velocity of the incoming wind (m/s)

v. Moment Coefficient

It is a dimensionless parameter that determines how efficient and effective the turbine blades are in utilizing the incoming wind speed to produce torque. It is given as;

$$Cm = \frac{Cp}{\lambda} \quad (9)$$

2.3 CFD Modelling Assumptions and Limitations of 2D CFD for a 3D Phenomenon

The CFD simulations were based on standard assumptions, which include a 2D approximation, incompressible flow (due to low Mach number), isotropic turbulence modelled using SST k-ω, no-slip boundary conditions, and uniform steady inflow. These assumptions reduce computational cost but limit accuracy by neglecting 3D effects such as tip losses, spanwise flow, and wake interactions. As a result, 2D simulations may overpredict lift and torque, especially under yawed or non-uniform inflow conditions. Therefore, the results should be validated with 3D CFD or experimental data.

2.4 Validation of Theoretical Trends with Previous Studies

Chord length has a major impact on VAWT performance, according to earlier research. Low Reynolds numbers and laminar separation bubbles decrease efficiency at low chord-to-diameter ratios, as demonstrated by Ma'alouly *et al.* (2022). According to Castelli *et al.* (2015), at high TSRs, increasing the chord can decrease the power coefficient even though it increases torque. The existence of an ideal solidity range for maximizing Cp was highlighted by Islam *et al.* (2008).

These results emphasize how crucial it is to carefully consider chord length in relation to TSR, wind conditions, and performance objectives.

3. MATERIALS AND METHOD

3.1. Description of the Geometry, Domain and Boundary condition

The NACA 0015 airfoil was employed for this study's VAWT, due to its high efficiency in small scale VAWTs. In order to determine the optimal chord length of NACA 0015 to employ in low wind speed regions, three chord lengths (0.1m, 0.2m and 0.3m) were investigated across a TSR that ranges from 2 to 4.5 with an increment of 0.5. The performance metrics of these three VAWT configurations analyzed were power output, power coefficient (Cp) and the Moment coefficient (Cm). In order to eliminate any interference by the boundaries, a large enough stationary domain (20D x 20D) was used for all the simulations. The stationary and rotating domain used by this study is shown in figure 1. The boundary condition used by this study can be seen in Table 1.

Table 1: Boundary Condition

Name	Boundary Condition
Inlet	Velocity In-let
Outlet	Pressure Outlet
Top	Zero specified shear stress
Bottom	Zero specified shear stress
Turbine Blades	No-Slip Condition

Table 2: VAWT Parameter

Name	Boundary Condition
Rotor Diameter	2m
Chord length	0.1m, 0.2m and 0.3m
Airfoil profile	NACA 0015
Number of Blade	3
Turbine Solidity	0.15, 0.3 and 0.45
Wind Speed	3m/s and 4m/s

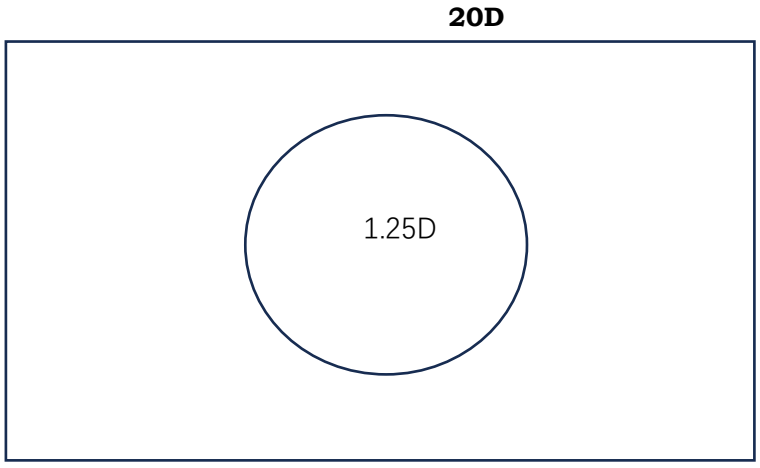

Figure 1: Stationary and Rotating Domain

3.2. Meshing

The all-triangular element size was employed for the two domains. So as to ensure a finer mesh around the turbine blades, the body of influence (BOI) around the turbine blades was made to have an element size of 0.003m. After which an inflation layer was applied on the blades. This is to ensure that the effect of boundary layers is accurately captured. The generated mesh can be seen in figure 2-4. High-quality meshes with local refinement were generated near the blade surfaces and boundary layers to ensure accurate resolution of critical flow features. Mesh quality metrics such as skewness, aspect ratios, element quality, and orthogonal quality were kept within the accepted range. A grid independence study was conducted using three mesh sizes as shown in table 3, in order to determine the accuracy of the mesh used by this study. Since the difference in efficiencies (Cp and Cm) between the medium and fine mesh was less than 2%, the medium-density mesh was adopted for all simulations to balance accuracy and computational cost.

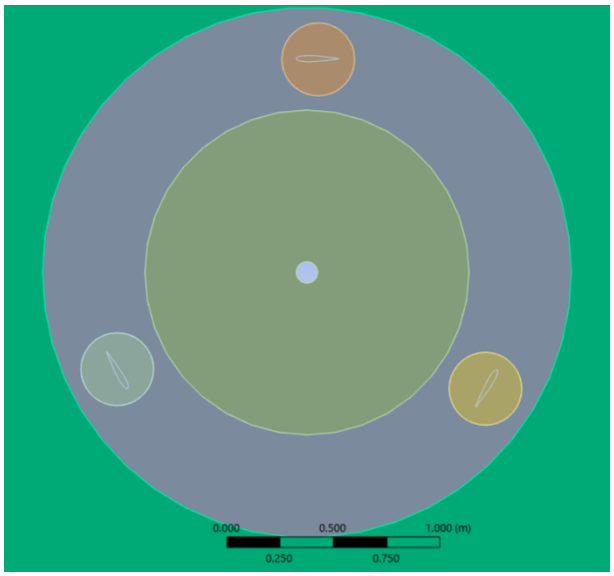

Figure 2: BOI around the Turbine blades

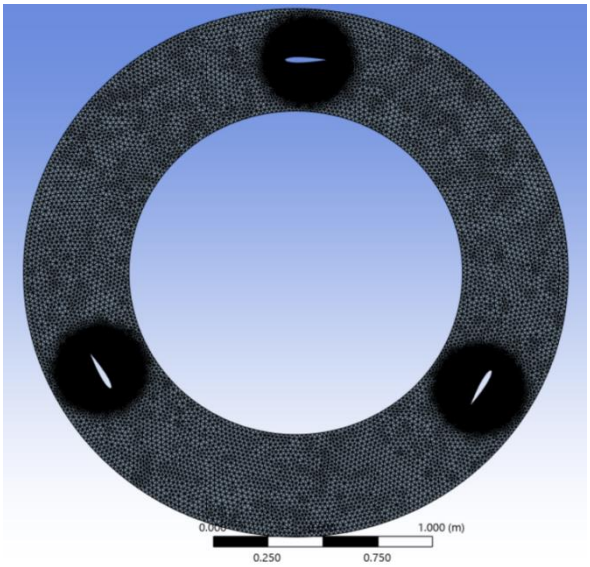

Figure 3: Meshed Rotating Domain and the BOI

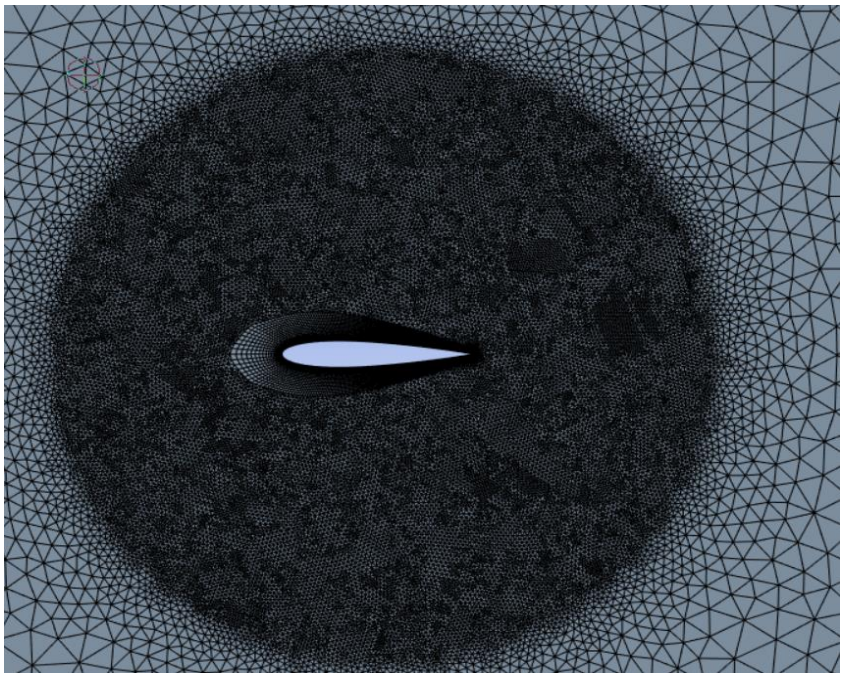

Figure 4: Meshed Turbine Blade

Table 3: Grid Independence Study

Grid Size	Mesh Element Count	Cp	Cm
Coarse	125,435	0.2	0.1
Medium	271,416	0.15	0.075
Fine	402, 749	0.145	0.0725

3.3. Numerical Simulation

The ANSYS Fluent 2024 R2 version was used to simulate the flow around the VAWT. A pressure-based solver was employed and in order to accurately predict the unsteady aerodynamic characteristics that VAWT are subjected to in real-world scenario, a transient simulation was performed for all the VAWT configurations tested. The turbulence model employed was the shear stress transport (SST) k-omega, because of its ability in accurately capturing the wall effect. This study employed the sliding mesh approach for its simulation and the pressure-velocity coupling used was the Semi Implicit Method for Pressure Linked Equation (SIMPLE).
The simulation was run for about 4,000 number of time step and 20 maximum iteration per time step was specified. The time step size used by this study was calculated using the equation below.

$$\Delta T = \frac{\pi}{\omega \, x \, 180} \qquad (10)$$

Where; ΔT = Time step size
ω = Angular speed of the turbine blades

3.4 Physical Time and Convergence Assessment

The transient simulation was conducted with a time step size calculated using Equation 10 and covered a total of 4000 time steps. The turbine was allowed to complete at least 10 full revolutions, ensuring that the unsteady flow characteristics had fully developed and reached a periodic or statistically stable behavior. This duration was chosen to eliminate transient startup effects and to allow meaningful extraction of performance parameters. Residuals were monitored throughout the simulation to assess numerical convergence. For each time step, the residuals for continuity and velocity components consistently dropped below 10^{-4}, confirming the stability and accuracy of the solution. The convergence history can be seen in figure 5-7.

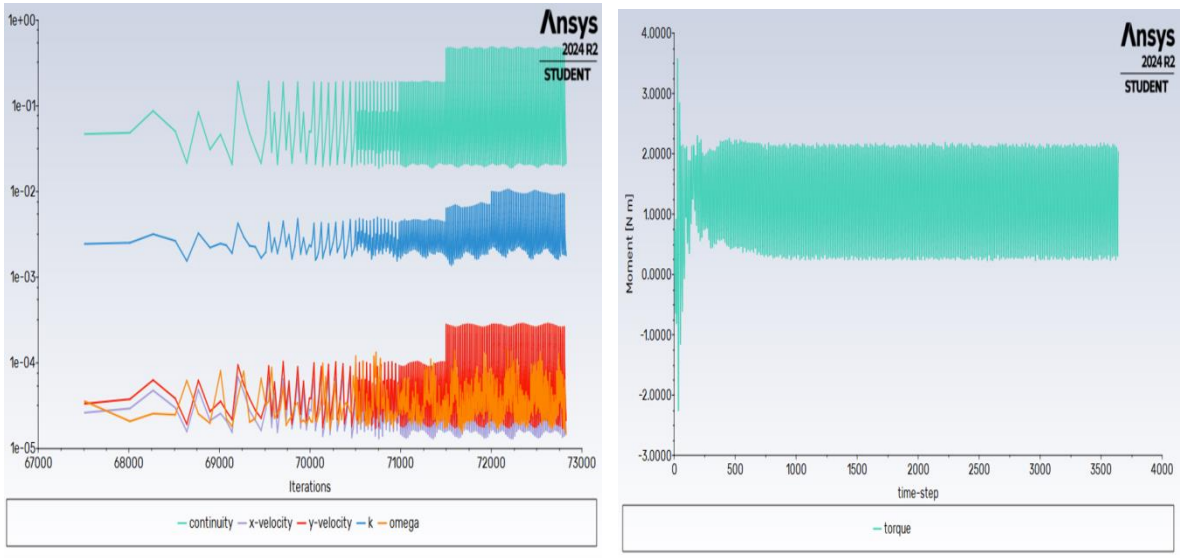

Figure 5: Residual and Torque Graph of NACA 0015 at chord length, c=0.1m

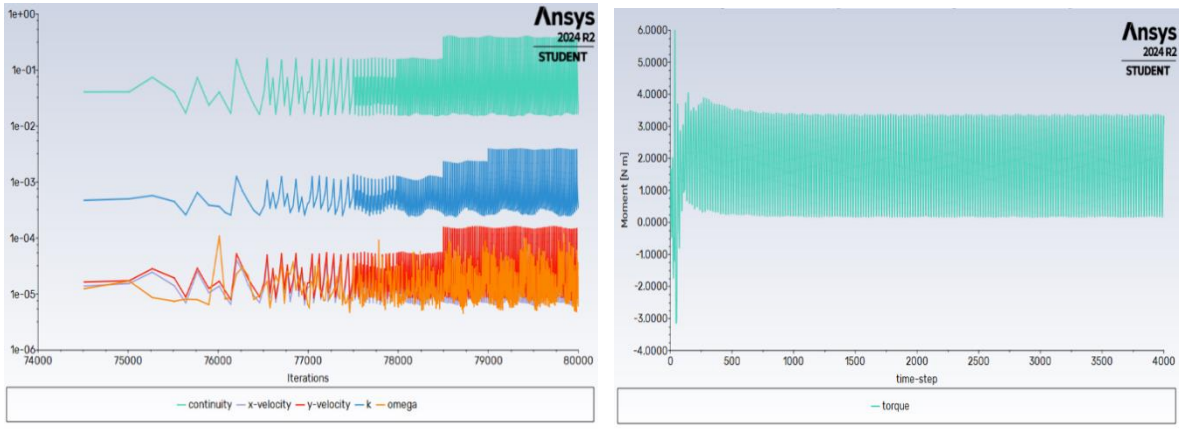

Figure 6: Residual and Torque Graph of NACA 0015 at chord length, c=0.2m

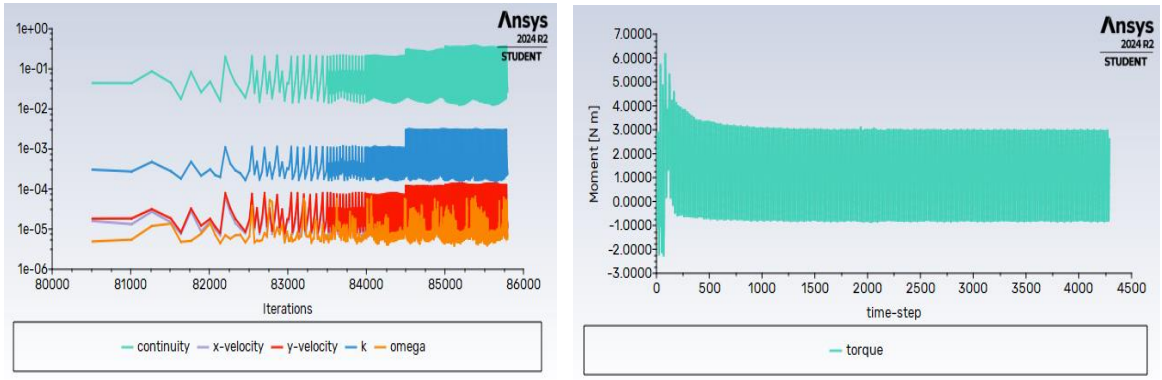

Figure 7: Residual and Torque Graph of NACA 0015 at chord length, c=0.3m

4. RESULTS AND DISCUSSION

The aerodynamic performance of the NACA 0015-based VAWT was evaluated under two low wind conditions (3 m/s and 4 m/s), using three chord lengths: 0.1 m, 0.2 m, and 0.3 m. The performance was evaluated using the power coefficient (Cp) and moment coefficient (Cm) across a range of Tip Speed Ratios (TSR) from 2.0 to 4.5. The goal was to determine how varying chord length influences energy capture in low-wind urban environments.

4.1 Performance at a wind speed of 4m/s

The 0.1m chord length yielded a peak Cp of 0.395 at a TSR of 4 as shown in figure 8, while the 0.2m chord length obtained its peak Cp value of 0.371 at a TSR of 3 as shown in figure 9. The maximum Cp achieved by the 0.3m chord length occurred at a TSR of 2.5 as shown in figure 10. It was later observed that operating the 0.3m chord length configuration beyond its peak TSR, will result to a sharp decline in power output which will eventually lead the turbine to the Dead band region (negative power output) at a TSR of 4. It can be observed from figure 11, that while the 0.1m chord length configuration has the highest Cp among the three-chord length tested, the 0.2m chord length configuration achieved its own peak Cp at a lower TSR, which is beneficial for operations in low wind speed environments.

The 0.2m chord length configuration was also observed to be more effective and efficient in generating more torque than the remaining two configurations. The moment coefficient achieved by the 0.2m chord length configuration at its optimal TSR was 0.124, while the configuration with the highest power output (0.1m chord length configuration), yielded a Cm value of 0.09875 at its optimal TSR. The combined Cm plot can be seen in figure 12.

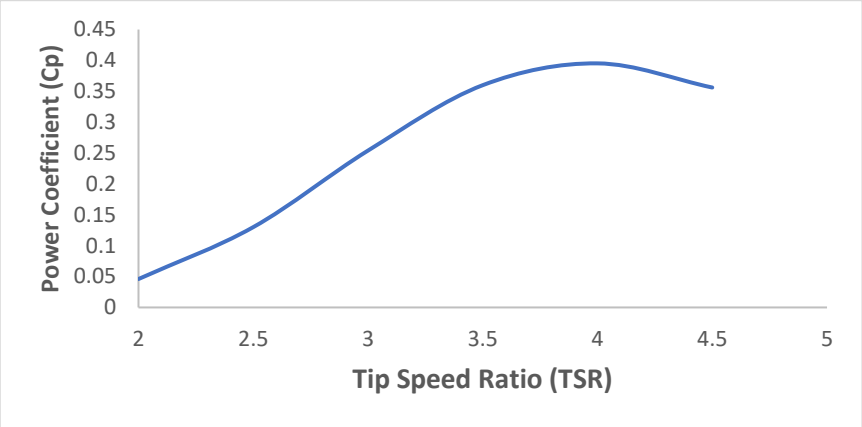

Figure 8: A graph of Cp Vs TSR for the 0.1m chord length configuration

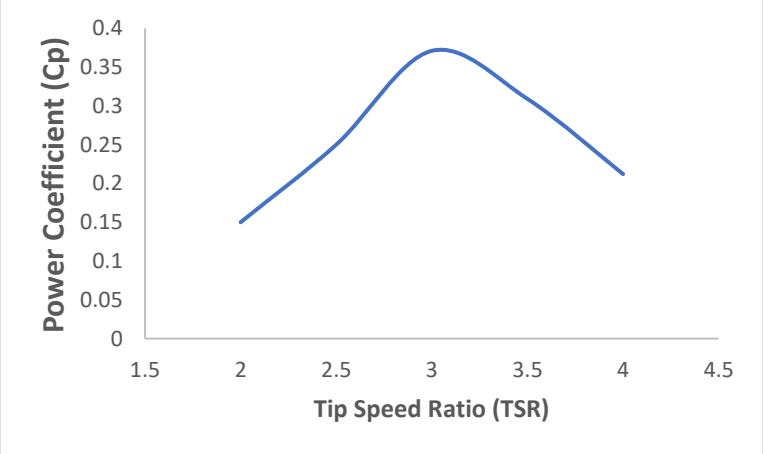

Figure 9: A graph of Cp Vs TSR for the 0.2m chord length configuration

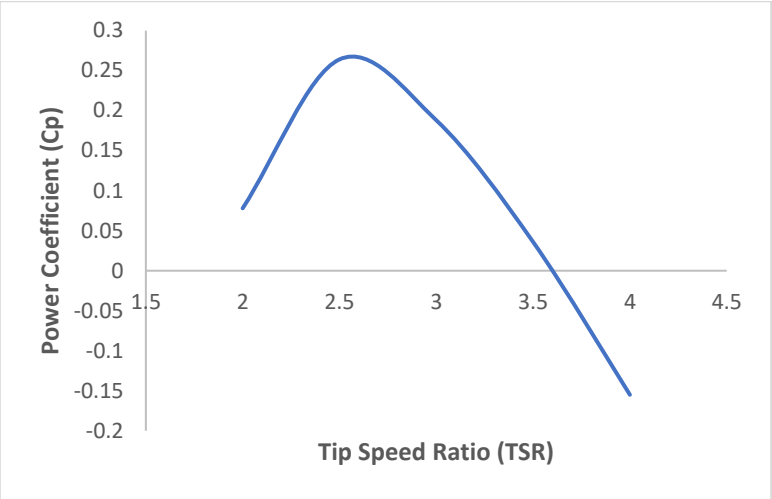

Figure 10: A graph of Cp Vs TSR for the 0.3m chord length configuration

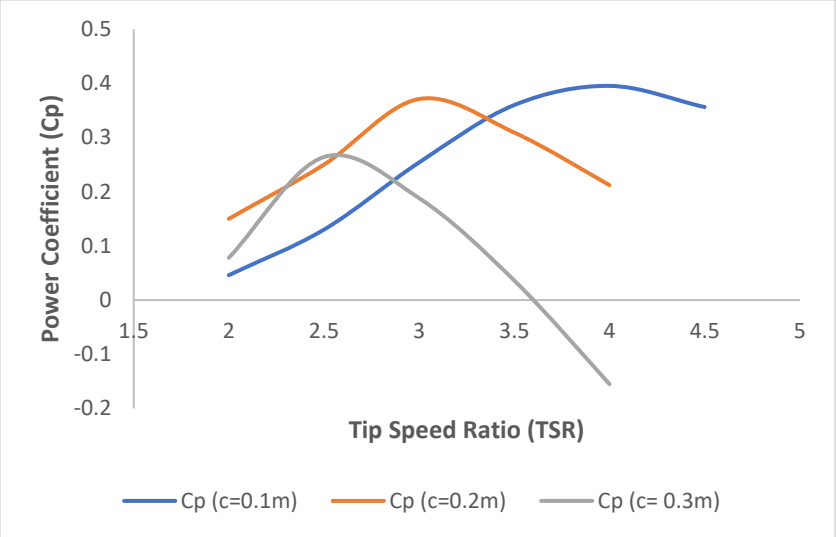

Figure 11: A Combined graph of Cp Vs TSR for all the configuration at the 4m/s wind speed

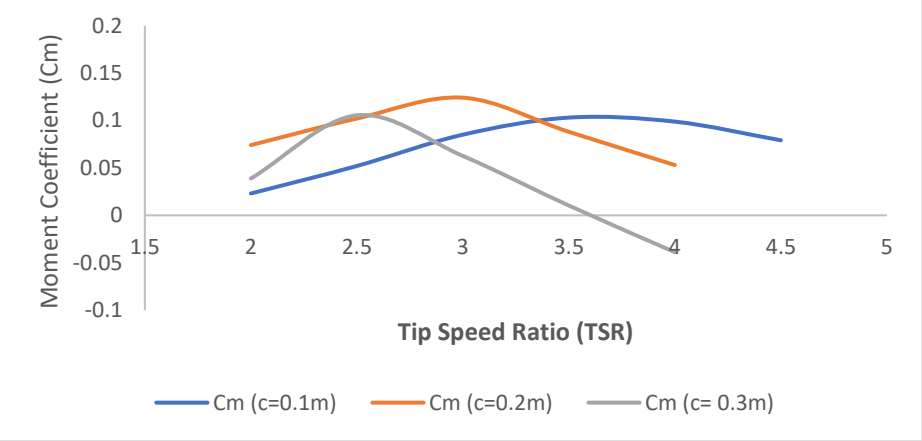

Figure 12: A Combined graph of Cm Vs TSR for all the configurations

4.2 Performance at a wind speed of 3m/s

At the lower wind speed of 3 m/s, the 0.2 m chord again delivered the highest performance, reaching a peak Cp=0.410, at TSR = 2.5 (see Figure 14). This highlights the chord's aerodynamic robustness even under reduced energy availability. The torque coefficient also followed a stable trend, pointing to effective energy extraction and minimal unsteady effects. The 0.1 m chord performed reasonably well, with a maximum Cp=0.337 at TSR = 3 (Figure 13). However, its curve exhibited a slower rise in Cp, confirming that it requires higher TSR to operate efficiently. This makes it less suited for low TSR conditions typical in irregular wind environments. The 0.3 m chord length again showed weak performance, peaking at Cp=0.279 and dropping to Cp=−0.540 at TSR = 4 (Figure 15). The torque and power curves reflect severe aerodynamic stall and flow separation, consistent with over-solidity effects.

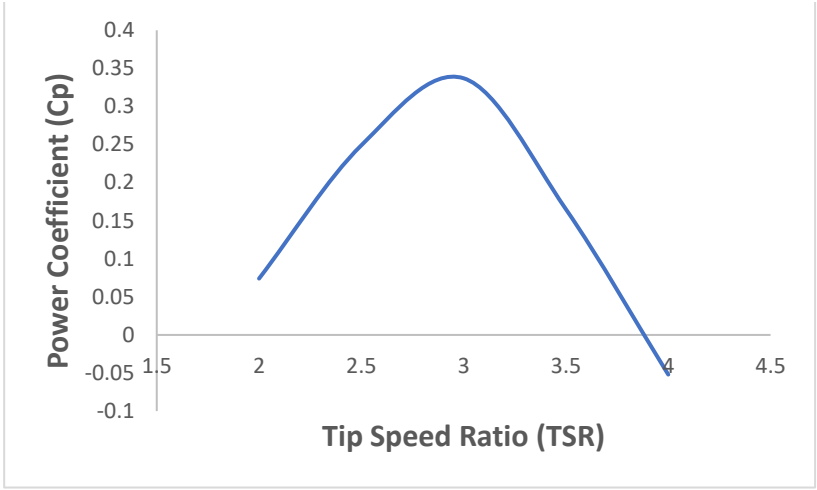

Figure 13: A graph of Cp Vs TSR for the 0.1m chord length configuration

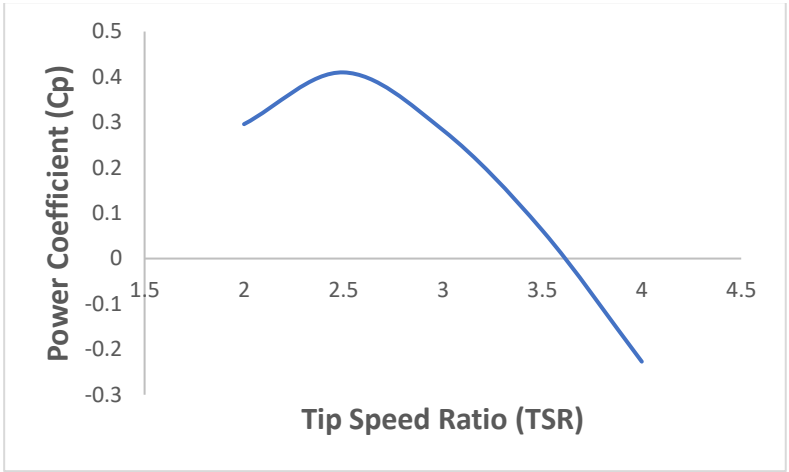

Figure 14: A graph of Cp Vs TSR for the 0.2m chord length configuration

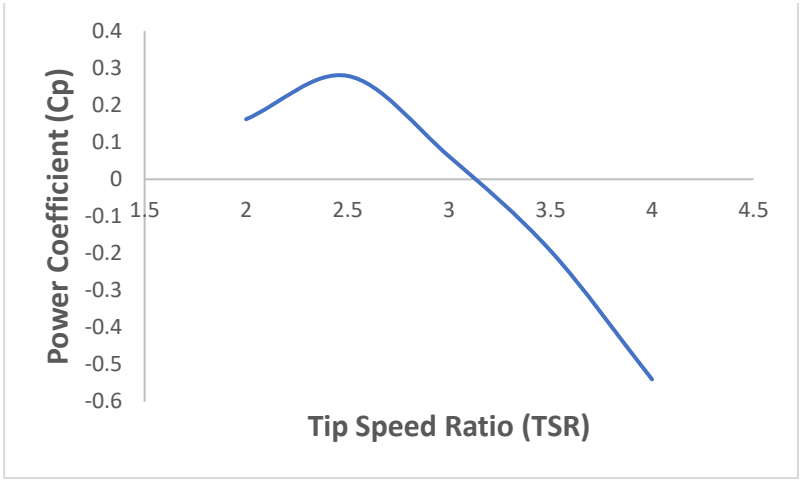

Figure 15: A graph of Cp Vs TSR for the 0.3m chord length configuration

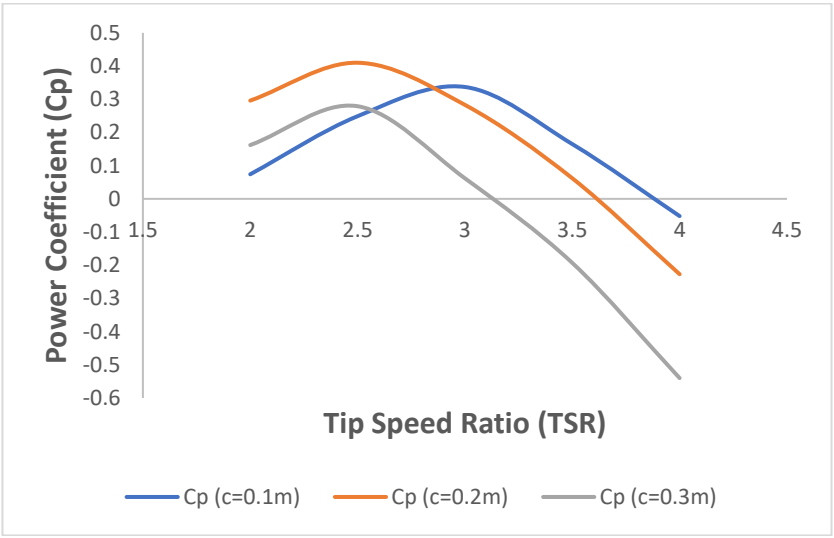

Figure 16: A Combined graph of Cp Vs TSR for all the configuration at the 3m/s wind speed

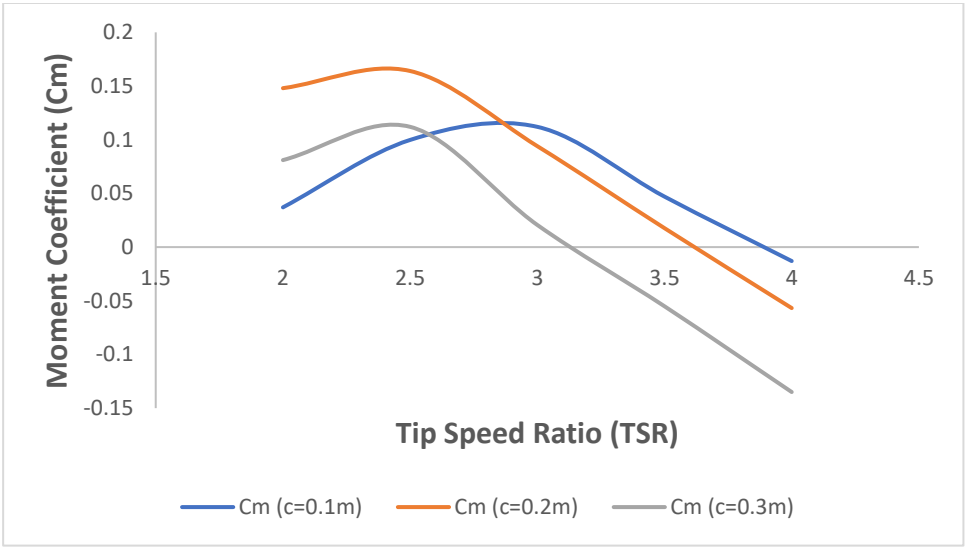

Figure 17: A Combined graph of Cm Vs TSR for all the configuration at the 3m/s wind speed

Hence, the results demonstrate that chord length directly influences not only peak performance but also operational stability under varying wind conditions. For urban or rooftop environments, where wind conditions are typically weak and unsteady, the 0.2 m chord configuration provides the most consistent and efficient performance, making it ideal for small-scale VAWT installations.

4.3 Aerodynamic Effects of Chord Length: Flow Visualization at 0.2 m and 0.3 m

The comparison between the NACA 0015 airfoil at chord lengths of 0.2 m and 0.3 m revealed a decline in aerodynamic performance. Velocity contours show that at the shorter chord (0.2 m), the flow accelerates more effectively over the airfoil surface, creating a stronger suction region and enhancing lift. In contrast, the 0.3 m chord displayed slower acceleration and broader low-velocity zones, particularly near the trailing edge, indicating early flow separation and less effective suction. This reduced surface velocity gradient results in a weaker pressure differential across the airfoil. Combined with greater boundary layer growth, stronger vorticity, and a larger wake, the 0.3 m configuration experiences more drag and less efficient lift generation, explaining the observed reduction in Cp and overall aerodynamic performance. The velocity, pressure and vorticity contour of the turbine blades at 0.2 m and 0.3 m chord length are shown in figures 18 – 23.

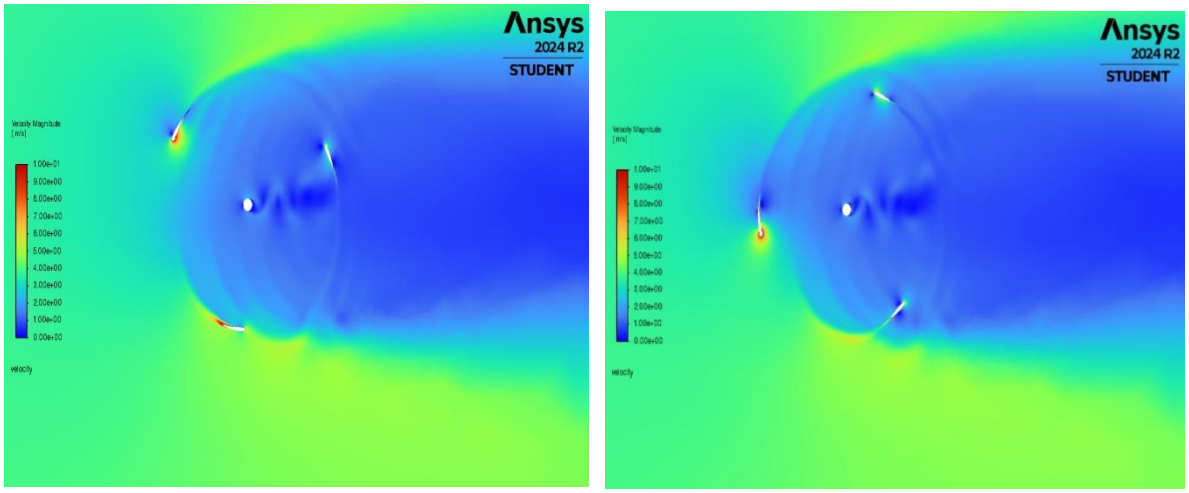

Figure 18: Velocity Contour of NACA 0015 at a chord length of 0.2m

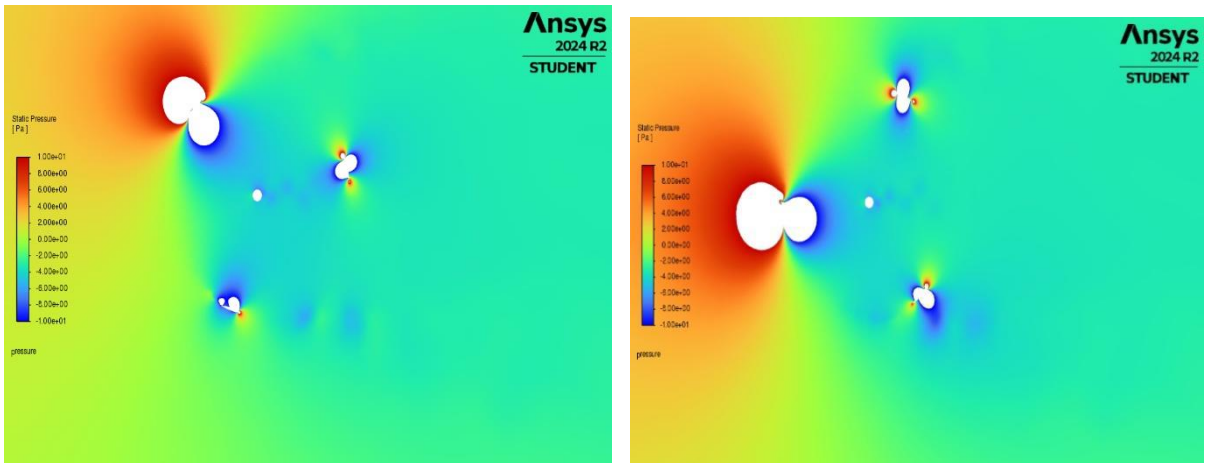

Figure 19: Pressure Contour of NACA 0015 at a chord length of 0.2m

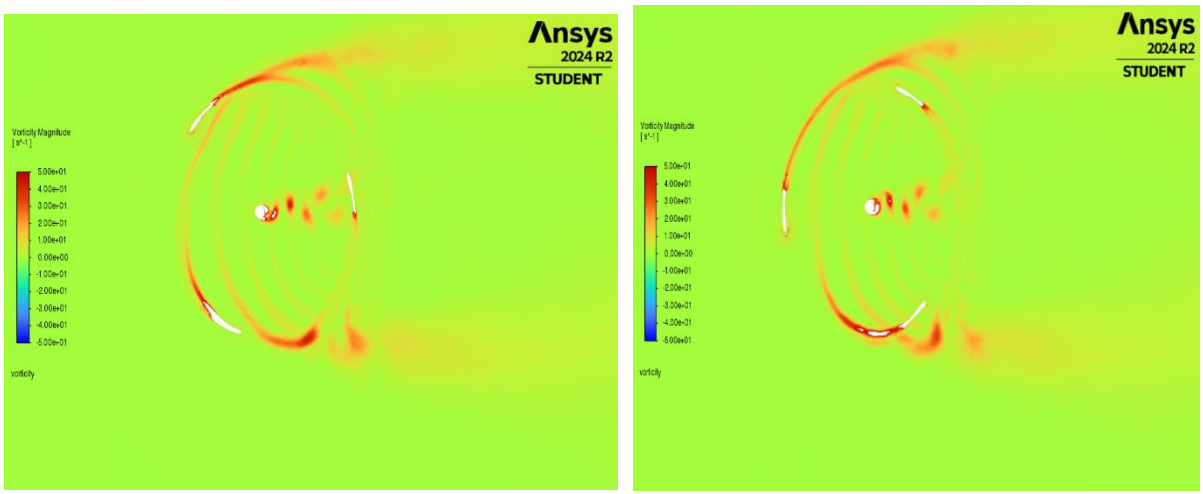

Figure 20: Vorticity Contour of NACA 0015 at a chord length of 0.2m

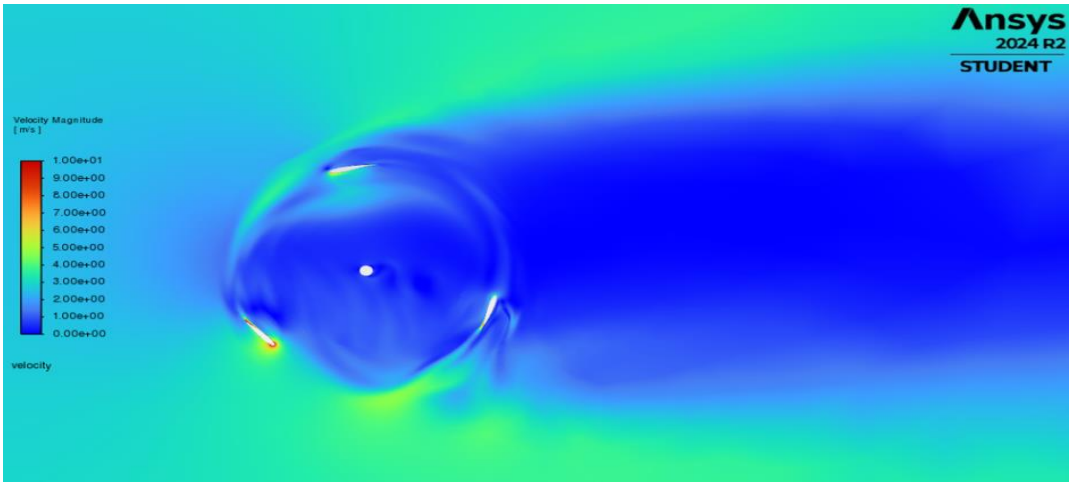

Figure 21: Velocity Contour of NACA 0015 at a chord length of 0.3m

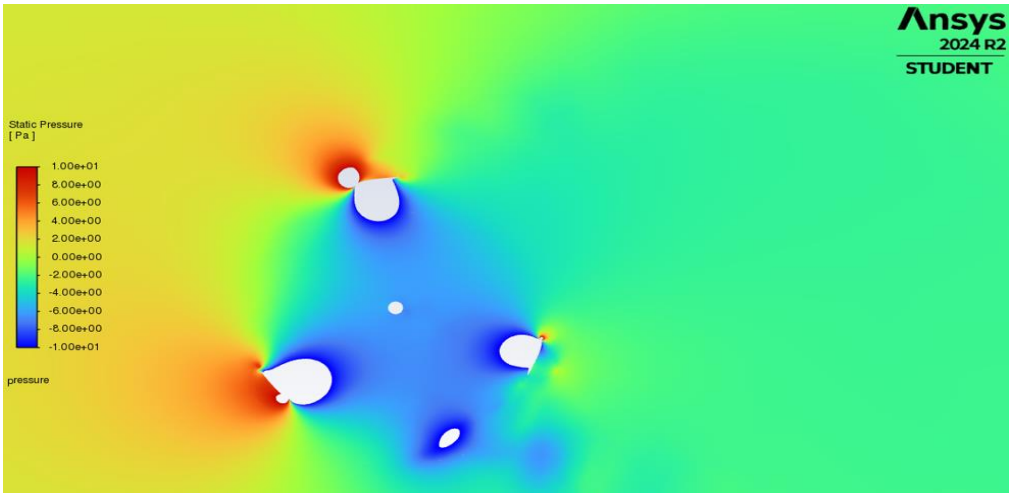

Figure 22: Pressure Contour of NACA 0015 at a chord length of 0.3m

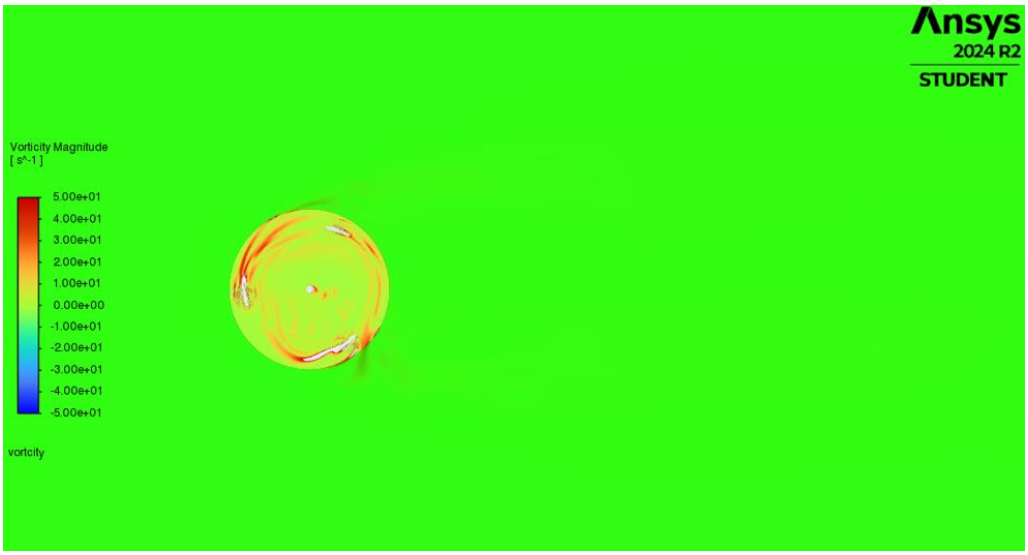

Figure 23: Vorticity Contour of NACA 0015 at a chord length of 0.3m

4.4 Result Validation

A validation study was performed to determine the accuracy of this study's simulation results. An agreement was found with the study conducted by Subramanian *et al.,* (2017), where a Cp value of 0.373 at a TSR of 2.2 was recorded for the VAWT. The study conducted by Mohamed *et al* (2014)**,** obtained a maximum Cp of 0.38 at a TSR of 3.8 for the VAWT with NACA 0015 airfoil. Hence, it can be concluded that the Cp obtained by this present study is within the acceptable range of Cp for a VAWT.

Table 4: Error Analysis of Simulated vs. Reference Cp Values for NACA 0015 Airfoil (Chord Length 0.2 m)

S/N	TSR	Cp (Mohamed *et al.,*)	Cp (This Study)
1	2	0.01	0.15
2	3	0.14	0.37
3	4	0.38	0.212

Two statistical tools used to quantify the deviation between simulated and reference Cp values were the root mean square error (RMSE) and mean bias error (MBE). The RMSE and MBE were calculated using Equations (11) and (12), respectively:

$$\text{RMSE} = \sqrt{\frac{1}{n}\sum_{i=0}^{n}(Pi - Qi)^2} \qquad (11)$$

$$\text{MBE} = \frac{1}{n}\sum_{i=0}^{n}(Pi - Qi) \qquad (12)$$

An RMSE value of **0.18** and an MBE value of **0.067** indicate that the results of this study deviate moderately from those reported by Mohamed *et al.* (2014). This deviation is attributed to differences in chord length and wind velocity between the two studies.

5. CONCLUSION AND RECOMMENDATION

5.1 Conclusion

This study has demonstrated that blade chord length plays a critical role in the aerodynamic performance of Vertical Axis Wind Turbines (VAWTs) operating under low wind conditions. Through 2D transient CFD simulations of a NACA 0015 airfoil at wind speeds of 3 m/s and 4 m/s, three chord lengths (0.1 m, 0.2 m, and 0.3 m) were evaluated. The results revealed that the 0.1 m chord length delivered the highest power output of 30.98 W with a peak power coefficient of Cp=0.3952 at TSR 4 for the 4 m/s wind speed. However, the 0.2 m chord length exhibited more stable and consistent performance, peaking at 29.11 W and Cp=0.371 at TSR 3. At 3 m/s

wind speed, the 0.2 m chord length again outperformed other configurations with a peak Cp=0.410 at TSR 2.5. In contrast, the 0.3 m chord length experienced early performance deterioration due to excessive solidity, producing negative Cp values at higher TSRs and exhibiting flow separation behavior supported by torque and lift trends. From a design perspective, the results strongly indicate that the 0.2 m chord length offers the best aerodynamic balance for VAWTs intended for low-wind urban environments, combining good power output with stable performance over a wide range of TSRs. This makes it a strong candidate for small-scale or rooftop wind energy systems in areas with moderate wind variability.

5.2 **Recommendation**

This study contributes to existing knowledge by providing an insight into how chord length variations affect the aerodynamic performance of NACA 0015-based VAWTs under low wind speed conditions. It reveals that a 0.2 m chord length offers the best trade-off between power coefficient stability, and flow separation control, especially in low-Reynolds-number regimes. The findings offer practical design insight for small-scale VAWTs in urban environments. Despite the insights gained, the findings are constrained by the limitations of 2D CFD modelling, which neglect spanwise flow effects, tip losses, and 3D wake interactions. These simplifications may impact the accuracy of torque and force predictions, especially near stall regions. As such, future studies should incorporate 3D CFD simulations and experimental validation to strengthen the reliability and applicability of the conclusions. Further studies should also explore other low-speed airfoil profiles, assess Reynolds number sensitivity, and evaluate the combined effects of chord length and pitch control strategies for enhanced aerodynamic efficiency.

REFERENCES

Bangga, G., Hutani, S., & Heramarwan, H. (2021). The effects of airfoil thickness on dynamic stall characteristics of high-solidity vertical axis wind turbines. Advanced Theory and Simulations. https://doi.org/10.1002/adts.202000204

Beri, H., & Yao, Y. (2012). Steady and unsteady computational analysis of vertical axis wind turbine. Proceedings of the Asia-Pacific Power and Energy Engineering Conference, 978. https://doi.org/10.1109/appeec.2012.6307139

Castelli, M. R., De Betta, S., & Benini, E. (2012). Effect of blade number on a straight-bladed vertical-axis Darreius wind turbine. World Academy of Science, Engineering and Technology International Journal of Aerospace and Mechanical Engineering, 6(1).

Davari, H. S., Botez, R. M., Davari, M. S., Chowdhury, H., & Hosseinzadeh, H. (2024). Numerical and experimental investigation of Darrieus vertical axis wind turbines to enhance self-starting at low wind speeds. Results in Engineering, 24, 103240. https://doi.org/10.1016/j.rineng.2024.103240

Danao, L. A., Luo, Y., & Howell, R. (2014). Investigation of the influence of blade profile on vertical axis wind turbine performance. Applied Energy, 107, 395–404. https://doi.org/10.1016/j.apenergy.2013.02.030

De Tavernier, D., Ferreira, C., Vir_e, A., LeBlanc, B., & Bernardy, S. (2021). Controlling dynamic stall using vortex generators on a wind turbine airfoil. Renewable Energy, 173, 1194–1211. https://doi.org/10.1016/j.renene.2021.03.019

Du, L., Ingram, G., & Dominy, R. G. (2019). Experimental study of the effects of turbine solidity, blade profile, pitch angle, surface roughness, and aspect ratio on the H-Darrieus wind turbine self-starting and overall performance. Energy Science & Engineering, 7(6), 2421–2436. https://doi.org/10.1002/ese3.430

Eboibi, O., Danao, L. M., & Howell, R. J. (2016). Experimental investigation of the influence of solidity on the performance and flow field aerodynamics of vertical axis wind turbines at low Reynolds numbers. Renewable Energy, 92, 474–483. https://doi.org/10.1016/j.renene.2016.02.028

Howell, R., Qin, N., Edwards, J., & Durrani, N. (2010). Wind tunnel and numerical study of a small vertical axis wind turbine. Renewable Energy, 35(2), 412–422. https://doi.org/10.1016/j.renene.2009.07.025

IEA. (2021). World Energy Outlook 2021. International Energy Agency. https://www.iea.org/reports/world-energy-outlook-2021

Islam, M., Ting, D. S. K., & Fartaj, A. (2013). Aerodynamic models for Darrieus-type straight-bladed vertical axis wind turbines. Renewable and Sustainable Energy Reviews, 12(4), 1087–1109. https://doi.org/10.1016/j.rser.2006.10.023

Kishore, R. A., Mishra, A., & Singh, S. N. (2021). Effect of solidity on the performance of vertical axis wind turbines. Energy Reports, 7, 2935–2945. https://doi.org/10.1016/j.egyr.2021.05.017

Lee, Y. T., & Lim, H. C. (2015). Numerical study of the aerodynamic performance of a 500 W Darrieus-type vertical-axis wind turbine. Renewable Energy, 83, 407–415. https://doi.org/10.1016/j.renene.2015.04.043

Li, Q., Maeda, T., Kamada, Y., Murata, J., Furukawa, K., & Yamamoto, M. (2015). Effect of number of blades on aerodynamic forces on a straight-bladed vertical axis wind turbine. Energy, 1–12. https://doi.org/10.1016/j.energy.2015.07.115

Maalouly, J., Al Rifai, M., Ramadan, M., & Khalil, R. A. (2022). Transient analysis of H-type vertical axis wind turbines using computational fluid dynamics. Energy Reports, 8, 2186–2201. https://doi.org/10.1016/j.egyr.2022.01.186

Maalouly, J., Hajj, M. R., & Nasr, A. (2022). Transient analysis of H-type VAWTs using CFD. Energy Reports, 8, 1901–1913. https://doi.org/10.1016/j.egyr.2022.01.021

Manwell, J. F., McGowan, J. G., & Rogers, A. L. (2010). Wind energy explained: Theory, design and application (2nd ed.). Wiley.

Mohamed, M. H., Ali, A. M., & Hafiz, A. A. (2014). CFD analysis for H-rotor Darrieus turbine as a low speed wind energy converter. Engineering Science and Technology, an International Journal, 1–13. https://doi.org/10.1016/j.jestch.2014.08.002

Paraschivoiu, I. (2002). Wind turbine design: With emphasis on Darrieus concept. Presses inter Polytechnique.

Ren21. (2022). Renewables 2022 global status report. https://www.ren21.net/reports/global-status-report/

Sebastien, F. L., & Karen, M. (2022). The dynamic stall dilemma for vertical-axis wind turbines. Renewable Energy, 505–520. https://doi.org/10.1016/j.renene.2022.07.071

Subramanian, A., Yogesh, S. A., Sivanandan, H., Giri, A., Vasudevan, M., Mugundhan, V., & Velamati, R. K. (2017). Effect of airfoil and solidity on performance of small-scale vertical axis wind turbine using three dimensional CFD model. Energy, 133, 179–190. https://doi.org/10.1016/j.energy.2017.05.118

Zhang, Y., Guo, Z., Song, X., Zhu, X., Cai, C., & Li, Q. (2021). Investigating of flow field and power performance on a straight-blade vertical axis wind turbine with CFD simulation. Journal of Energy Research and Reviews, 9(1), 32–42. https://doi.org/10.9734/jenrr/2021/v9i130223